Memory effects for a trapped Brownian particle in viscoelastic shear flows

Romi Mankin, Katrin Laas,* and Neeme Lumi
Institute of Mathematics and Natural Sciences, Tallinn University, 29 Narva Road, 10120 Tallinn, Estonia
(Received 19 July 2013; published 28 October 2013)

The long-time limit behavior of the positional distribution for an underdamped Brownian particle in a fluctuating harmonic potential well, which is simultaneously exposed to an oscillatory viscoelastic shear flow is investigated using the generalized Langevin equation with a power-law-type memory kernel. The influence of a fluctuating environment is modeled by a multiplicative white noise (fluctuations of the stiffness of the trapping potential) and by an additive internal fractional Gaussian noise. The exact expressions of the second-order moments of the fluctuating position for the Brownian particle in the shear plane have been calculated. Also, shear-induced cross correlation between particle fluctuations along orthogonal directions as well as the angular momentum are found. It is shown that interplay of shear flow, memory, and multiplicative noise can generate a variety of cooperation effects, such as energetic instability, multiresonance versus the shear frequency, and memory-induced anomalous diffusion in the direction of the shear flow. Particularly, two different critical memory exponents have been found, which mark dynamical transitions from a stationary regime to a subdiffusive (or superdiffusive) regime of the system. Similarities and differences between the behaviors of the models with oscillatory and nonoscillatory shear flow are also discussed.

DOI: 10.1103/PhysRevE.88.042142 PACS number(s): 05.40.−a, 02.50.−r, 83.50.Ax

I. INTRODUCTION

Recent years have witnessed an increasing interest in noise-induced phenomena in nonequilibrium dynamical systems. Stochastic fluctuations often evoke an unexpected response in physical, chemical, and biological systems; these include stochastic resonance [1,2], noise-enhanced stability [3,4], hypersensitive response [5,6], and the ratchet effect [7,8], to name a few. Specifically, anomalous diffusion with the mean-square displacement of particles $\langle r^2(t)\rangle \sim t^\alpha (\alpha \neq 1)$ is found in different systems [9–18]. Examples of such systems are supercooled liquids, glasses, colloidal suspensions, polymer solutions [9,10], amorphous semiconductors, viscoelastic media [11,12,19], cytoplasm of living cells [20], and large proteins [21].

One of the possibilities for modeling anomalous diffusion in physical and biological systems can be formulated in the framework of the generalized Langevin equation (GLE) [13,15–17]. In most cases a GLE is obtained by replacing the usual Stokes-type friction term by a generalized friction term with a power-law memory [13–17]. Physically such a friction term has, due to the fluctuation-dissipation theorem [22], its origin in a non-Ohmic thermal bath, whose influence on the dynamical system is described with a power-law correlated additive internal noise in the GLE, e.g., with fractional Gaussian noise, which is closely related to fractional Brownian motion [13,16].

Although the behavior of Brownian motion in quiescent fluids has been investigated in detail, our understanding of thermally induced particle dynamics in flows is still far from complete [23,24]. Especially in shear flows, little is known about the dynamics of Brownian particles and about hydrodynamic interaction effects in spite of their fundamental relevance and importance in microfluidic applications [23,25–27]. Of particular interest are small mesoscopic systems such as colloidal particles, nanoparticles in solutions, or biological systems in cells, all of which are dominated by fluctuations. Recently, to overcome part of this problem, several studies have focused on the dynamics of underdamped Brownian particles trapped by harmonic potentials and exposed to shear flows [23,24,28–30]. The interest in harmonically trapped particles has been stimulated by new experimental techniques to trap mesoscopic particles, such as laser-optical tweezers [31,32], which allow direct observation and manipulation of individual particles under the influence of external forces of flows (see also Ref. [23], and references therein).

It should be noted that Refs. [23,24,28,29] consider shear flows independent of time, but in Ref. [30] the response of Brownian particles to an externally imposed oscillatory shear flow is explored. The analytical solutions exposed in Ref. [30] reveal that in weakly damped systems both the particle and velocity distributions and the cross moments exhibit a strong resonance. With relatively low shear rates, it is possible to induce a significant anisotropy in the distribution functions. Potential experiments to verify those theoretical results on dusty plasmas and trapped colloidal dispersions in a fluid solvent are also discussed in Ref. [30].

However, in Refs. [23,24,28–30] it is assumed that the interaction of Brownian particles with shear flow is characterized by Stokes friction. The latter is irrelevant for shear flow in viscoelastic media, where anomalous diffusion occurs. Moreover, the previous calculations are based on models without using multiplicative noise. It is important to note that multiplicative noise in GLE arises in a natural way in quantitative measurements with laser-optical tweezers, where the stiffness of the effective trapping potential may fluctuate [31].

Motivated by the results of Ref. [30], the present paper considers a model similar to the one presented in Ref. [30], except that the Stokes-type friction term is replaced with a power-law-type memory kernel and that the influence of the fluctuating environment is modeled not by additive Gaussian white noise, but by a multiplicative white noise (fluctuating

*katrin.laas@tlu.ee

 ©2013 American Physical Society

stiffness of the effective trapping potential) and by an additive internal fractional noise.

The main contribution of this paper is as follows. In the long-time limit, ($t \to \infty$), we provide exact formulas for the analytic treatment of the dependence of second-order moments of the fluctuating particle position and the mean angular momentum of the rotational part of particle motion in the shear plane on system parameters, such as the shear oscillation frequency, the memory exponent, the shear rate, the intensity of the multiplicative noise, and the friction coefficient. We show that although the stochastic motion of a trapped particle moving in oscillatory shear flow with a characteristic oscillation frequency Ω and of a particle in time-independent shear flow ($\Omega = 0$) have common characteristic signatures, such as an inclined elliptical particle distribution, there are also substantial differences. Specifically, it is found that the critical memory exponents, which mark dynamical transitions from a stationary regime to an anomalous diffusive regime of the system, are different for the cases $\Omega \neq 0$ and $\Omega = 0$. This effect is due to the involvement of different time scales in the models. To avoid misunderstandings, let us mention that we use the term stationary regime in a wide sense, meaning bounded (also periodic) first and second moments of output by increasing time. Furthermore, we show that in the case of $\Omega \neq 0$, in certain parameter regions the second-order moment of the particle displacement in the direction of the shear flow exhibits a multiresonance behavior versus Ω. We also demonstrate that the presence of multiplicative noise in the GLE has a profound effect on the behavior of the particle distribution: first, as the intensity of the multiplicative noise tends to a critical value, energetic instability appears, which makes a stationary regime impossible; second, in the vicinity of the critical intensity the particle distribution is very much elongated in the shear flow direction in comparison with the case without multiplicative noise.

Moreover, for fractional dynamics with memory we have derived Eqs. (14) and (40), which can be useful for calculations of the correlators for fractional dynamics with multiplicative white noise (Appendix C).

The structure of the paper is as follows. In Sec. II we present the model investigated. Exact formulas are found for the analysis of the behavior of the second-order moments and of the mean angular momentum. In Sec. III we analyze the dependence of the particle distribution characteristics on system parameters. Section IV contains some brief concluding remarks. Some formulas and proofs are delegated to the Appendixes.

II. MODEL AND THE EXACT MOMENTS

A. Model

We consider a Brownian particle of the unit mass ($m = 1$) suspended at the position $\boldsymbol{r} = (X,Y,Z)$ in a viscoelastic flow field with parallel streamlines in the x direction

$$\boldsymbol{v}(\boldsymbol{r},t) = \rho Y \cos(\Omega t)\mathbf{e}_x, \tag{1}$$

with $\mathbf{e}_x$ denoting the unit vector in the x direction, ρ the shear rate, and Ω the shear frequency. The particle is trapped by a harmonic potential with its minimum at $\boldsymbol{r}_0 = 0$,

$$U(\boldsymbol{r}) = \frac{\omega^2}{2}\boldsymbol{r}^2, \tag{2}$$

where ω is the trap frequency. As a model for such a system with memory, strongly coupled with a noisy environment, we consider a GLE with a fluctuating harmonic confinement potential $\tilde{U}(\boldsymbol{r})$

$$\ddot{\boldsymbol{r}}(t) + \gamma \int_0^t \eta(t-t')\{\dot{\boldsymbol{r}}(t') - \boldsymbol{v}[\boldsymbol{r}(t'),t']\}dt' + \nabla\tilde{U}(\boldsymbol{r}) = \boldsymbol{\xi}(t), \tag{3}$$

where $\dot{\boldsymbol{r}} \equiv d\boldsymbol{r}/dt$, γ is the damping coefficient, and $\boldsymbol{\xi}(t) = [\xi_1(t),\xi_2(t),\xi_3(t)]$ is the internal Gaussian stochastic force. The latter is assumed to have zero mean, $\langle\boldsymbol{\xi}(t)\rangle = 0$, and the stationary power-law correlation function

$$\langle\xi_i(t)\xi_j(t')\rangle = \frac{\gamma k_B T \delta_{ij}}{\Gamma(1-\alpha)|t-t'|^\alpha}. \tag{4}$$

Here, T is the absolute temperature of the heat bath, k_B is the Boltzmann constant, and $\Gamma(1-\alpha)$ is the gamma function. The memory exponent α can be taken as $0 < \alpha < 1$, which is determined by the viscoelastic properties of the medium. Since the driving noise $\boldsymbol{\xi}(t)$ is internal noise, the memory kernel $\eta(t)$ in Eq. (3) satisfies Kubo's second fluctuation-dissipation theorem [22] expressed as

$$\gamma k_B T \eta(|t-t'|)\delta_{ij} = \langle\xi_i(t)\xi_j(t')\rangle. \tag{5}$$

By taking the limit $\alpha \to 1$ in Eqs. (4) and (5) we see that the correlation function (4) possesses all properties of δ function (its δ-functional behavior manifests itself in the integrals) and thus the noise $\boldsymbol{\xi}(t)$ corresponds to white noise and consequently, to nonretarded friction in the GLE (3) [16,17,33]. It should be noted that the internal noise $\boldsymbol{\xi}(t)$ with the power-law correlation function (4) has been successfully applied in the description of a wide variety of problems in viscoelastic media [13–17,34]. The fluctuating confinement potential $\tilde{U}(\boldsymbol{r})$ is assumed to be in the form

$$\tilde{U}(\boldsymbol{r}) = U(\boldsymbol{r}) + \frac{X^2}{2}Z_1(t) + \frac{Y^2}{2}Z_2(t) + \frac{Z^2}{2}Z_3(t), \tag{6}$$

where $\boldsymbol{Z}(t) = [Z_1(t),Z_2(t),Z_3(t)]$ is a white noise with the following properties:

$$\langle\boldsymbol{Z}(t)\rangle = 0, \quad \langle Z_i(t)Z_j(t')\rangle = 2D\delta_{ij}\delta(|t-t'|),$$
$$\langle Z_i(t_1)\dots Z_i(t_n)\rangle = \langle Z_i(t_1)Z_i(t_2)\rangle\langle Z_i(t_3)\dots Z_i(t_n)\rangle, \tag{7}$$

where $t_1 \geqslant t_2 \geqslant \cdots \geqslant t_n$, and D is the noise intensity (cf. also Ref. [35]). Although we assume a special type of the white noise with properties (7), the results discussed in this paper are more general. For example, all results do not change if the noises $Z_i(t)$ are replaced with Gaussian white noises (see Appendix C). The noise $\boldsymbol{Z}(t)$ is assumed as statistically independent from the noise $\boldsymbol{\xi}(t)$. In the following we use the Stratonovich interpretation of the GLE (3) with a fluctuating confinement potential (6). Note that such a potential acting, for example, on a colloidal particle may be realized by optical tweezers [31,32]. It should be pointed out that in the case of Stokes friction ($\alpha = 1$) and without the multiplicative noise $\boldsymbol{Z}(t)$ the model (3) reduces to the model for a trapped Brownian

particle in an oscillatory shear flow previously considered in [30]. Due to the linearity of the restoring force, $-\nabla\tilde{U}(\boldsymbol{r})$, the z component in Eq. (3) decouples and remains–by sufficiently small intensities of the multiplicative noise $\boldsymbol{Z}(t)$, $D < D_{cr}$–in equilibrium

$$\langle Z(t)\rangle = 0, \quad \langle Z^2\rangle = \frac{k_B T D_{cr}}{\omega^2(D_{cr} - D)}. \tag{8}$$

Therefore, in the rest of this paper we consider the motion in the x-y plane. The occurrence and the behavior of the critical noise intensity D_{cr} are established in Sec. II C (cf. also Refs. [36,37]).

Note that counterparts of the model (3) without the multiplicative noise $\boldsymbol{Z}(t)$ and flow field $\boldsymbol{v}(\boldsymbol{r},t)$ are widely used in fitting experimental data from intracellular microrheology and from single-molecule experiments probing conformational fluctuations in proteins (see, e.g., Refs. [13,14,38]). For example, in Ref. [14] the authors succeeded in modeling the motion of the donor-acceptor distance within a protein as the coordinate of a fictitious particle diffusing in a harmonic potential according to a GLE [i.e., with the help of a model similar to Eq. (3) with $\boldsymbol{Z}(t) = \boldsymbol{v}(\boldsymbol{r},t) = 0$], while the memory exponent $\alpha \approx 0.51$ was deduced from experimental observations.

B. First moments

In the x-y plane, the GLE (3) can be written as two second-order fractional differential equations

$$\ddot{Y}(t) + \gamma\frac{d^\alpha}{dt^\alpha}Y(t) + [\omega^2 + Z_2(t)]Y(t) = \xi_2(t), \tag{9}$$

$$\ddot{X}(t) + \gamma\frac{d^\alpha}{dt^\alpha}X(t) + [\omega^2 + Z_1(t)]X(t) = \xi_1(t) + \gamma\rho\frac{d^\alpha}{dt^\alpha}\left[\int_0^t Y(t')\cos(\Omega t')dt'\right], \tag{10}$$

where the operator d^α/dt^α with $0 < \alpha < 1$ denotes the fractional derivative in Caputo's sense, given by [33]:

$$\frac{d^\alpha f(t)}{dt^\alpha} = \frac{1}{\Gamma(1-\alpha)}\int_0^t \frac{\dot{f}(t)}{(t-t')^\alpha}dt'. \tag{11}$$

After averaging Eqs. (9) and (10) over the ensemble of realizations of the random processes $\boldsymbol{Z}(t)$ and $\boldsymbol{\xi}(t)$ we obtain

$$\frac{d^2}{dt^2}\langle Y(t)\rangle + \gamma\frac{d^\alpha}{dt^\alpha}\langle Y(t)\rangle + \omega^2\langle Y(t)\rangle = 0, \tag{12}$$

$$\frac{d^2}{dt^2}\langle X(t)\rangle + \gamma\frac{d^\alpha}{dt^\alpha}\langle X(t)\rangle + \omega^2\langle X(t)\rangle = \gamma\rho\frac{d^\alpha}{dt^\alpha}\left[\int_0^t \langle Y(t')\rangle\cos(\Omega t')dt'\right]. \tag{13}$$

Here we have used that from Eqs. (3) and (7) it follows that the correlator

$$\langle \boldsymbol{Z}(t)\boldsymbol{r}(t)\rangle_Z = 0, \tag{14}$$

where $\langle\rangle_Z$ denotes an average over an ensemble of realizations of the multiplicative noise. A proof of the last statement is given in Appendix C. Thus, it turns out that fluctuations of the confinement potential do not affect the first moments $\langle X(t)\rangle$ and $\langle Y(t)\rangle$ of the output of the GLE, provided the fluctuations are δ-correlated, and $\langle \boldsymbol{r}(t)\rangle$ remains equal to the noise-free solution. By applying the Laplace transformation to Eqs. (9) and (10) one can easily obtain formal expressions for the displacements $X(t)$ and $Y(t)$ in the following forms:

$$Y(t) = \langle Y(t)\rangle + \int_0^t H(t-\tau)[\xi_2(\tau) - Y(\tau)Z_2(\tau)]d\tau, \tag{15}$$

$$X(t) = \langle X(t)\rangle + \int_0^t H(t-\tau)\left\{\xi_1(\tau) - X(\tau)Z_1(\tau) + \gamma\rho\frac{d^\alpha}{d\tau^\alpha}\left[\int_0^\tau (Y(t') - \langle Y(t')\rangle)\cos(\Omega t')dt'\right]\right\}d\tau, \tag{16}$$

where the averages $\langle Y(t)\rangle$ and $\langle X(t)\rangle$ are given by

$$\langle Y(t)\rangle = \dot{y}_0 H(t) + y_0 G(t), \tag{17}$$

$$\langle X(t)\rangle = \dot{x}_0 H(t) + x_0 G(t) + \gamma\rho\int_0^t \left\{H(t-\tau) \times \frac{d^\alpha}{d\tau^\alpha}\left[\int_0^\tau \langle Y(t')\rangle\cos(\Omega t')dt'\right]\right\}d\tau, \tag{18}$$

with the deterministic initial conditions $X(0) = x_0$, $Y(0) = y_0$, $\dot{X}(0) = \dot{x}_0$, and $\dot{Y}(0) = \dot{y}_0$. The relaxation functions $H(t)$ and $G(t)$ with the initial conditions $H(0) = 0$ and $G(0) = 1$ are the Laplace inversions of

$$\hat{H}(s) = \int_0^\infty e^{-st}H(t)dt = \frac{1}{s^2 + \gamma s^\alpha + \omega^2}, \tag{19}$$

$$\hat{G}(s) = \frac{s + \gamma s^{\alpha-1}}{s^2 + \gamma s^\alpha + \omega^2}, \tag{20}$$

respectively. Integral representations of the relaxation functions $H(t)$ and $G(t)$ are given by Eqs. (A1)–(A8) in Appendix A. For large t the functions $H(t)$ and $G(t)$ decay as power law, namely, at $t \to \infty$

$$H(t) \sim t^{-(1+\alpha)}, \quad G(t) \sim t^{-\alpha}. \tag{21}$$

Thus, in the long-time limit, $t \to \infty$, in Eq. (17) the memory about the initial conditions will vanish and the average y-coordinate $\langle Y(t)\rangle_{as} := \langle Y(t)\rangle_{|t\to\infty}$ is zero, i.e.,

$$\langle Y(t)\rangle_{as} = 0. \tag{22}$$

The asymptotic behavior of the average displacement in the x direction, $\langle X(t)\rangle_{as}$, is more subtle. It follows from Eqs. (17)–(20) that we have two different cases. (i) An oscillatory shear flow, $\Omega \neq 0$. In this situation, if t is much larger than $1/\Omega$, then $\langle X(t)\rangle$ tends to zero as

$$\langle X(t)\rangle \sim t^{-\alpha}, \quad t \to \infty, \quad \Omega \neq 0. \tag{23}$$

(ii) The static limit, $\Omega = 0$. In this case we get

$$\langle X(t)\rangle \sim y_0 t^{1-2\alpha}, \quad t \to \infty, \quad \Omega = 0, \quad y_0 \neq 0. \tag{24}$$

Thus (recall that $y_0 \neq 0$), the asymptotic value $\langle X(t)\rangle_{as} = 0$ if the memory exponent α is in the interval $(1/2, 1)$. On the other hand, if $\alpha < 1/2$, the average displacement $\langle X(t)\rangle$ grows unlimited as $\langle X(t)\rangle \sim t^{1-2\alpha}$. Therefore, in the case $\Omega = 0$, $y_0 \neq 0$, $\alpha < 1/2$ relaxation to a stationary regime is not possible.

C. Second moments

In the following, our interest is in the stationary regime in the long-time limit, $t \to \infty$, when the system has lost all memory of the initial conditions. We consider the second moments $\langle X^2(t)\rangle$, $\langle Y^2(t)\rangle$, and $\langle X(t)Y(t)\rangle$ that determine the particle's positional distribution function (see Refs. [23,24,28–30]). Here we remind the reader that we use the term "stationary regime" in a wide sense, meaning bounded (also periodic) first and second moments of output by increasing time.

Since the motion in the y direction is independent of the shear flow and of the motion in the x -direction, the respective correlation functions and also the moment $\langle Y^2(t)\rangle$ remain unaffected. They are simply those of a fractional oscillator with fluctuating frequency and can be found as in Refs. [36,37]. In particular, in the long-time limit

$$\langle Y(t+\tau)Y(t)\rangle_{as} = \frac{k_B T}{\omega^2} G(\tau) + 2D\langle Y^2\rangle_{as}\psi(\tau), \tag{25}$$

$$\langle Y^2\rangle_{as} = \frac{k_B T D_{cr}}{\omega^2(D_{cr}-D)}, \tag{26}$$

where

$$\psi(\tau) := \int_0^\infty H(t)H(t+\tau)dt, \tag{27}$$

$$D_{cr} = [2\psi(0)]^{-1}. \tag{28}$$

From Eq. (26) we can see that the stationary regime is possible only if $D < D_{cr}$. The exact formula useful for a numerical treatment of the critical noise intensity D_{cr} is given by Eq. (A9) (see Appendix A). As the noise intensity D tends to the critical value D_{cr} the variance $\langle Y^2\rangle_{as}$ increases to infinity. This is an indication that for $D > D_{cr}$ energetic instability appears, which manifests itself in an unlimited increase of the second-order moments of the output of the oscillator with time, while the mean value of the oscillator displacement remains finite [35,39]. It is important to note that the formulas (25)–(28) are applicable for all values of the memory exponent, $0 < \alpha < 1$.

Using Eqs. (14), (16), and (25) we obtain

$$\langle X(t)Y(t)\rangle_{as} = \gamma\rho\langle Y^2\rangle_{as}\int_0^t \chi(t')F(t')\cos[\Omega(t-t')]dt', \quad t \to \infty, \tag{29}$$

where

$$F(t) := 2D\psi(t) + G(t)[1-2D\psi(0)], \tag{30}$$

$$\chi(t) := \frac{1}{\gamma}[G(t) - \dot{H}(t)]. \tag{31}$$

Equation (29) can be written as

$$\langle X(t)Y(t)\rangle_{as} = \gamma\rho\langle Y^2\rangle_{as}|A(\infty)|\cos(\Omega t + \varphi_1), \tag{32}$$

where

$$A(t) := \int_0^t \chi(t')F(t')e^{-i\Omega t'}dt', \tag{33}$$

and the phase shift φ_1 can be represented as

$$\tan\varphi_1 = \frac{\mathrm{Im}A(\infty)}{\mathrm{Re}A(\infty)}. \tag{34}$$

In the case of nonoscillatory shear flow, $\Omega = 0$, the integral (33) converges at $t \to \infty$ only if $\alpha > 1/2$. If the memory exponent $\alpha < 1/2$, then the cross correlation $\langle X(t)Y(t)\rangle$ grows unlimited as

$$\langle X(t)Y(t)\rangle \sim t^{1-2\alpha}, \quad \alpha < \tfrac{1}{2}, \quad \Omega = 0, \tag{35}$$

and a stationary regime is not possible [see also Eqs. (A19) and (A21) in Appendix A].

Next we consider, in the long-time limit, the behavior of the variance $\langle X^2(t)\rangle$. Suppose that the system has been relaxed to a stationary regime. Starting from Eqs. (16) and (25), we obtain the following asymptotic formula for the second moment of the particle displacement in the x direction

$$\langle X^2(t)\rangle_{as} = \langle Y^2\rangle_{as}\left\{1 + \gamma^2\rho^2\left[\frac{\mathrm{Re}(B_0)}{(1-2D\psi(0))} + \frac{|B_1|}{|1-2D\phi(\Omega)|}\cos(2\Omega t + \varphi_2)\right]\right\}, \tag{36}$$

where

$$B_j := \int_0^\infty [e^{(-1)^j i\Omega t_1}\chi(t_1)\int_0^{t_1} e^{-i\Omega t_2}\chi(t_2)F(t_1-t_2)]dt_2dt_1, \quad j = 0,1, \tag{37}$$

$$\phi(\Omega) := \int_0^\infty H^2(t)e^{2i\Omega t}dt, \tag{38}$$

and the phase shift φ_2 is given by

$$\tan\varphi_2 = -\frac{\mathrm{Im}[B_1(1-2D\phi(\Omega)]}{\mathrm{Re}[B_1(1-2D\phi(\Omega)]}. \tag{39}$$

Here we have used that because of the statistical independence of the processes $\boldsymbol{\xi}(t)$ and $\boldsymbol{Z}(t)$ it follows from Eq. (14) that (see Appendix C)

$$\langle \boldsymbol{\xi}(t_1)X(t_2)\boldsymbol{Z}(t_2)\rangle = \langle \boldsymbol{\xi}(t_2)X(t_1)\boldsymbol{Z}(t_1)\rangle = 0 \tag{40}$$

and that in the case of a δ-correlated noise $\boldsymbol{Z}(t)$ the correlator $\langle X(t_1)X(t_2)Z_1(t_1)Z_1(t_2)\rangle$ can be given by

$$\langle X(t_1)X(t_2)Z_1(t_1)Z_1(t_2)\rangle = 2D\langle X^2(t_2)\rangle\delta(|t_1-t_2|). \tag{41}$$

The exact formulas convenient for a numerical treatment of the quantities $A(\infty)$ and B_j are given by Eqs. (A12) and (A16) (see Appendix A).

In effect, the integral B_0, Eq. (37), converges to a finite value only if $\alpha > 1/2$ for the case of $\Omega \neq 0$ and if $\alpha > 2/3$ for $\Omega = 0$. Therefore, a stationary regime in the x direction is possible only if the above conditions are fulfilled. Particularly, it can be shown that in the case of $\Omega = 0$ and $\alpha < 2/3$, the second moment $\langle X^2(t)\rangle$ grows as $t^{2-3\alpha}$ for large t. In this case, the long-time behavior of the particle in the x direction is subdiffusive for $1/3 < \alpha < 2/3$ or superdiffusive if $\alpha < 1/3$. In the case of an oscillatory shear flow, $\Omega \neq 0$, the process $X(t)$ is subdiffusive for $\alpha < 1/2$, $\langle X^2(t)\rangle \sim t^{1-2\alpha}$.

In the case of Stokes friction, $\alpha = 1$, it is known that the flow leads to rotation in the x-y plane with an angular momentum $\langle L_z(t)\rangle = \langle X(t)\dot{Y}(t) - Y(t)\dot{X}(t)\rangle$, [28,30]. For the model (3), it is given by

$$\langle L_z(t)\rangle_{as} = -\rho\langle Y^2\rangle_{as}|C|\cos(\Omega t + \varphi_3), t \to \infty, \tag{42}$$

where

$$C = \gamma\int_0^\infty e^{-i\Omega t}[\chi(t)\dot{F}(t) - \dot{\chi}(t)F(t)]dt \tag{43}$$

and

$$\tan\varphi_3 = \frac{\mathrm{Im}C}{\mathrm{Re}C}. \tag{44}$$

It is remarkable that the formulas (42)–(44) are applicable for all values of the memory exponent, $0 < \alpha < 1$ [see also Appendix A, Eq. (A13)].

III. RESULTS

A. Time-independent shear flow

Several aspects of the behavior of a Brownian particle in time-independent shear flow with Stokes friction have been experimentally and theoretically investigated in Refs. [23,24,28,29,40]. In this section, we will focus on the case of a viscoelastic shear flow and explore the influence of multiplicative noise on the dynamics of a single particle.

1. Critical noise intensity

In Figs. 1(a) and 1(b) we depict the behavior of the critical noise intensity D_{cr} and the second moments $\langle X^2\rangle_{as}$, $\langle Y^2\rangle_{as}$, and $\langle XY\rangle_{as}$ by variations of the memory exponent α. Figure 1(a) shows a typical phenomenon of the memory-enhanced energetic stability considered previously in Ref. [37]. The dependence of D_{cr}/γ on α shows a typical

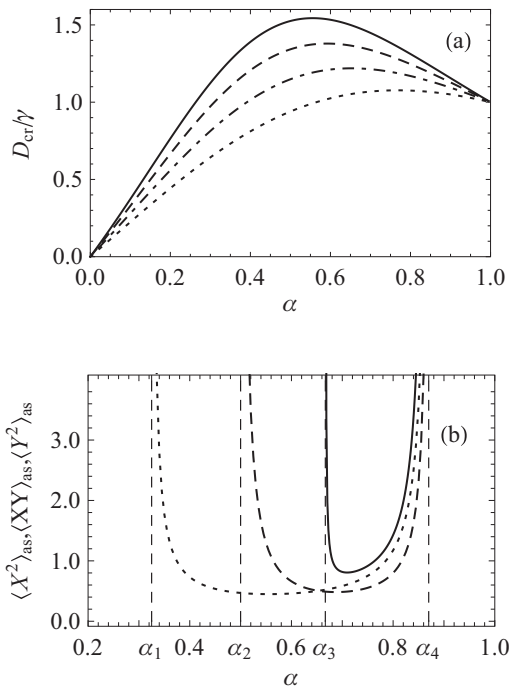

FIG. 1. Dependence of the critical noise intensity D_{cr} and the second moments computed from Eqs. (28), (A9), (26), (32), (A12), (36), and (A16) on the memory exponent α. Parameter values: $\omega = 1$, $\Omega = 0$, and $\rho = 0.03$. (a) D_{cr}/γ vs α at different values of the friction coefficient γ. Solid line: $\gamma = 4$; dashed line: $\gamma = 3$; dashed-dotted line: $\gamma = 2$; dotted line: $\gamma = 1$. (b) Second moments vs α. System parameter values: $k_BT = 0.1$, $D = 4.8$, and $\gamma = 4$. Solid line: $\langle X^2\rangle_{as}$; dashed line: $\langle XY\rangle_{as}$; dotted line: $\langle Y^2\rangle_{as}$. The thin dashed vertical lines mark the positions of the critical memory exponents: $\alpha_1 \approx 0.325$, $\alpha_2 = 1/2$, $\alpha_3 = 2/3$, $\alpha_4 \approx 0.872$.

resonance-like behavior of $D_{cr}(\alpha)$. As a rule, the maximal value of D_{cr}/γ increases as the value of the friction coefficient γ increases, while the positions of the maxima are monotonically shifted to lower α as γ rises. In the case considered in Fig. 1(b) the intensity of the multiplicative noise is in the interval $\omega^2\gamma < D < D_{\mathrm{crmax}}$, where D_{crmax} is the maximal value of $D_{cr}(\alpha)$ by variations of α. In this case the moments $\langle X^2\rangle_{as}$, $\langle Y^2\rangle_{as}$, and $\langle XY\rangle_{as}$ increase rapidly to infinity at α_4, $D_{cr}(\alpha_4) = D$. This is an indication that for $\alpha \geqslant \alpha_4$ energetic instability appears. From Fig. 1(b) it can be seen that there also occur three other critical memory exponents, $\alpha_1 \approx 0.325, \alpha_2 = 1/2$, and $\alpha_3 = 2/3$, at which the moments $\langle Y^2\rangle_{as}$, $\langle XY\rangle_{as}$, and $\langle X^2\rangle_{as}$ diverge, respectively. The critical exponent α_1, $D = D_{cr}(\alpha_1)$, indicates the occurrence of energetic instability for $\langle Y^2\rangle_{as}$ at α_1, but the critical exponents α_2 and α_3 characterize a transition from confined dynamics to a subdiffusive regime (see also Sec. II).

2. Distribution of particle position

If multiplicative noise is absent, the right-hand sides of Eqs. (15) and (16) are linear combinations of Gaussian processes $\boldsymbol{\xi}(t) = [\xi_1(t),\xi_2(t)]$, thus $\boldsymbol{r}(t) = [X(t),Y(t)]$ is also Gaussian and therefore completely specified by its mean and correlation matrix. So, in the long-time limit, $t \to \infty$, the stationary particle position distribution $P(\boldsymbol{r})$ is Gaussian (cf. Refs. [23,28]):

$$P(\boldsymbol{r}) = \frac{1}{\sqrt{(2\pi)^2 \det(\boldsymbol{M})}} \exp\left[-\frac{1}{2}\boldsymbol{r}^T \boldsymbol{M}^{-1}\boldsymbol{r}\right], \tag{45}$$

where the superscript "T" in Eq. (45) denotes transpose, and the covariance matrix $\boldsymbol{M}$ is given by

$$\boldsymbol{M} = \begin{pmatrix} \langle X^2\rangle_{as} & \langle XY\rangle_{as} \\ \langle XY\rangle_{as} & \langle Y^2\rangle_{as} \end{pmatrix}. \tag{46}$$

In the general case of Eq. (3), i.e., in the presence of a multiplicative noise and time-dependent shear flow, the particle distribution $P(\boldsymbol{r},t)$ is not necessarily Gaussian. However, in this work we also use the matrix $\boldsymbol{M}$ computed from Eqs. (26), (32), and (36) to characterize the particle distribution in the general case (cf. also Refs. [23,30]). If the positional distribution $P(\boldsymbol{r})$ is Gaussian (or approximately Gaussian), the nondiagonal elements of the matrix $\boldsymbol{M}$, cf. Eqs. (45) and (46), describe the cross correlations of the particle fluctuations in the x and y directions and, consequently, the deviation $P(\boldsymbol{r})$ from a spherically symmetric distribution to an ellipsoidal one in the shear plane. Thus the particle positional distribution is described by a covariance ellipsoid, with the lengths of its two main axes C_1 and C_2, which are given by the corresponding eigenvalues C_1^2 and C_2^2 of the matrix $\boldsymbol{M}$ (see Refs. [23,28], also Eq. (B2) in Appendix B). The larger main axis of the covariance ellipsoid forms an angle ϕ with the x axis [see Eq. (B3)], which starts out at $\pi/4$ for small shear rates ($\rho \to 0$) and approaches zero for large shear rates ($\rho \to \infty$), [28]. The behavior of the covariance ellipsoids by an increasing intensity D of the multiplicative noise are illustrated in Fig. 2. By increasing the noise intensity D both the ratio $V = C_2/C_1$ of the minor and the major axis of the covariance ellipsoid and the angle ϕ in Fig. 2 decrease monotonically. At the critical noise intensity, $D \to D_{cr}$, both characteristics V and ϕ tend

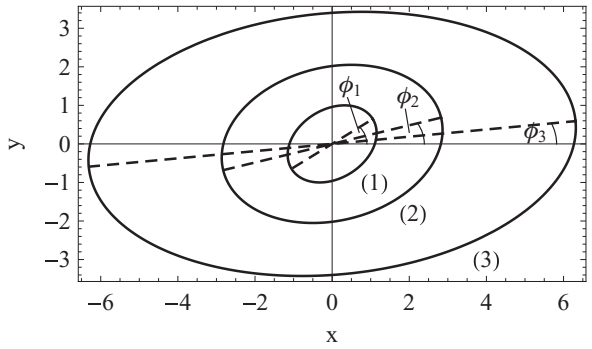

FIG. 2. The covariance ellipsoids in the x-y plane computed from Eqs. (26), (32), (36), (B2), and (B3) at $\Omega = 0$ for several values of the intensity D of the multiplicative noise. Parameter values: $\omega = 1$, $\rho = 0.1$, $k_BT = 1$, $\gamma = 4$, and $\alpha = 0.8$. Line (1): $D = 0$; line (2): $D = 4$; line (3): $D = 4.8$. The angles between the larger main axis and the x axis are: $\phi_1 = 0.5497$, $\phi_2 = 0.2368$, and $\phi_3 = 0.0934$.

to zero. This circumstance reflects the fact that the parametric stochastic resonance associated with energetic instability is more pronounced for $\langle X^2\rangle$ compared with the second moments $\langle Y^2\rangle$ and $\langle XY\rangle$, [cf. Eqs. (26), (32), and (36)].

In Fig. 3 we depict, on two panels, the behavior of $V(\alpha)$ and $\phi(\alpha)$ for various values of the noise intensity $D < D_{cr}(2/3)$. Both $V(\alpha)$ and $\phi(\alpha)$ exhibit a nonmonotonic dependence on the memory exponent α, i.e., a typical resonance phenomenon

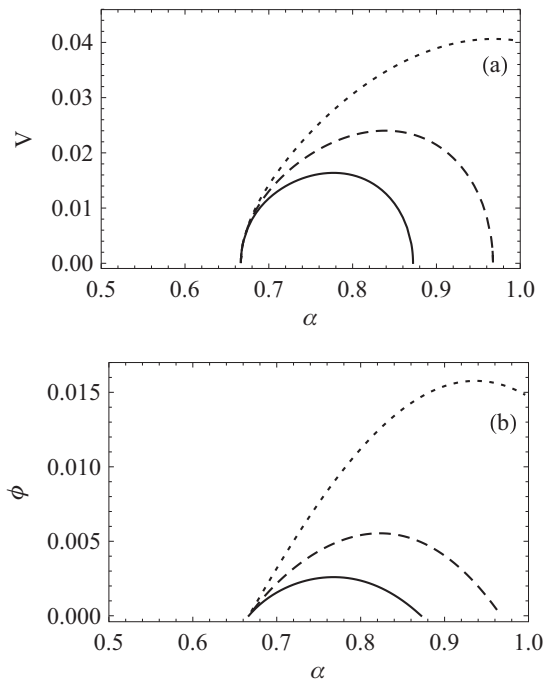

FIG. 3. The ratio $V = C_2/C_1$ of the minor and the major axis of the covariance ellipsoid and the angle ϕ between the major axis and x axis as functions on the memory exponent α. The curves are computed from Eqs. (26), (32), (36), (B2), and (B3) for several values of the multiplicative noise intensity D. Parameter values: $\Omega = 0$, $\rho = \gamma = 4$, $k_BT = \omega^2 = 1$. Solid line: $D = 4.8$, dashed line: $D = 4.2$; dotted line: $D = 3$. In the case of solid line, $D = 4.8$, the critical memory exponent α_1 equals to $\alpha_1 \approx 0.8721$.

occurs as α increases. Clearly, the resonancelike behavior of the covariance-ellipsoid characteristics versus α is significantly associated with the nonmonotonous dependence of the critical noise intensity $D_{cr}(\alpha)$ on the memory exponent and with the subdiffusive motion of a Brownian particle in the x direction at $\alpha < 2/3$. In the case of $\omega^2\gamma < D < D(2/3)$, the phenomenon of memory-induced resonance is very pronounced. In particular, in this case the system is in the stationary regime only if the values of the memory exponent are in the finite interval $\alpha \in (2/3,\alpha_1)$, $D = D_{cr}(\alpha_1)$; at $\alpha = 2/3$ the quantities V and ϕ tend to zero due to the appearance of subdiffusive dynamics in the x direction ($\langle X^2\rangle$ increases unlimited).

3. Time asymmetry in the cross correlation

Inspired by a recent experiment [40], where shear-induced cross correlations of particle position fluctuations perpendicular and along streamlines in the case of Stokes friction are investigated we now consider the behavior of the asymptotic cross-correlation functions $\langle X(t+\tau)Y(t)\rangle_{as}$ and $\langle X(t)Y(t+\tau)\rangle_{as}$, (see also Appendix A). As pointed out in Refs. [23,40], the shear-induced asymmetry of the cross-correlation functions $\langle X(t+\tau)Y(t)\rangle_{as} \neq \langle X(t)Y(t+\tau)\rangle_{as}$ with respect to the time lag τ is one of the important effects of shear flow on the distribution of particle positional fluctuations. The typical forms of the graphs $K_1(\tau)$ and $K_2(\tau)$ vs τ are represented in Fig. 4, where $K_1(\tau)$ and $K_2(\tau)$ are the normalized cross-correlation functions

$$K_1(\tau) = \frac{1}{\langle XY\rangle_{as}}\langle X(t+\tau)Y(t)\rangle_{as},$$
$$K_2(\tau) = \frac{1}{\langle XY\rangle_{as}}\langle Y(t+\tau)X(t)\rangle_{as}. \tag{47}$$

Note that the exact cross-correlation functions exhibit exponentially damped oscillations around a curve, which for large τ decay absolutely monotonically like a power law. Namely, both cross-correlation functions decay, in the long-time-lag regime as $\tau^{1-2\alpha}$ (see Appendix A). In a quiescent

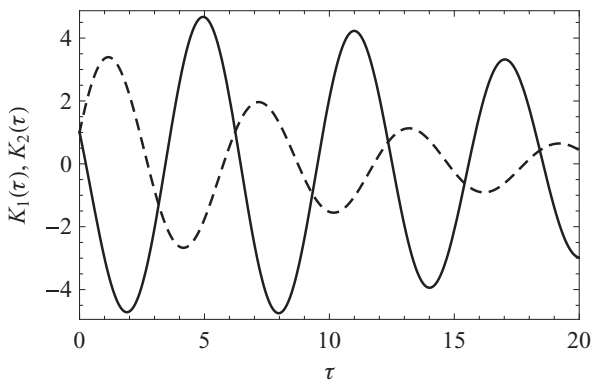

FIG. 4. Normalized cross-correlation functions $K_1(\tau)$ and $K_2(\tau)$ vs the time lag τ in the case of nonoscillatory shear flow, $\Omega = 0$. The curves are computed from Eqs. (47), (A22), and (A23). Parameter values: $\omega^2 = \rho = k_BT = 1$, $\gamma = 0.2$, $\alpha = 0.7$, and $D = 0.1$. The solid line and the dashed line correspond to the dependence of $K_1(\tau)$ and $K_2(\tau)$ on the time lag τ, respectively.

fluid cross correlations between particle displacements in orthogonal directions vanish, i.e., $\langle X(t+\tau)Y(t)\rangle_{as} = \langle Y(t+\tau)X(t)\rangle_{as} = 0$. But shear flow causes finite cross correlations in the shear plane [23,40].

In experimental realizations, the time lag is $\tau_{\min} \leqslant \tau \leqslant \tau_{\max}$, where $\tau_{\min}$ is the acquisition time interval and $\tau_{\max}$ is the measurement time. Therefore it is important to analyze the behavior of the correlation functions $K_1(\tau)$ and $K_2(\tau)$ for several time scales involved in the model (3). There are three important characteristic times for $K_i(\tau)$, $i = 1,2$:

$$\tau_1 = \frac{1}{\beta}, \tag{48}$$

$$\tau_2^{(2)} = \frac{2(2\alpha-1)DD_{cr}}{\omega^4(D_{cr}-D)}, \quad i = 2, \tag{49}$$

$$\tau_2^{(1)} = \left\{\tau_2^{(2)}\frac{\omega^2\Gamma(\alpha)}{\gamma\Gamma(2\alpha)[1-2\cos(\pi\alpha)]}\right\}^{\frac{1}{1-\alpha}}, \quad i = 1. \tag{50}$$

Below, we consider the case

$$\tau_{\min} < \tau_1 \ll \tau_2^{(i)} \ll \tau_{\max} \tag{51}$$

to allow the following separation of time scales: (i) $\tau \lesssim \tau_1$; (ii) $\tau_1 \ll \tau \ll \tau_2^{(i)}$; (iii) $\tau \gg \tau_2^{(i)}$. From Eq. (A3) it follows that τ_1 depends only on the parameters α, γ, and ω. Particularly, as a rule, τ_1 increases as γ or α decrease. Note that in the time region $\tau < \tau_1$ the oscillatory behavior of $K_1(\tau)$ and $K_2(\tau)$ is significant [see Fig. 4, cf. also Eqs. (A2), (A9), (A22), and (A23)] and thus it should be used in the interpretation of experimental results. Notably, the usually employed overdamped approximation is not applicable in this situation.

The other characteristic time $\tau_2^{(2)}$ is related to the asymptotic regimes of the correlation function $K_2(\tau)$ and is defined as the time at which a crossover from a power-law regime with the exponent -2α to a power-law regime with the exponent $1-2\alpha$ occurs (see Fig. 5). More precisely, at a long-time limit ($\tau \to \infty$) the asymptotic behavior of $K_i(\tau)$, $\alpha > 1/2$, is given by Eqs. (A24) and (A25), from which follow the formulas (49) and (50) for the characteristic times $\tau_2^{(i)}$. It is obvious that $\tau_2^{(2)}$ tends to a very large value in the vicinity of energetic instability, $D \to D_{cr}$. If $\tau_2^{(2)} > \tau_{\max}$, then the asymptotic monotonic decay of the correlation function $K_2(\tau)$ should be used with care in the interpretation of experimental data. Namely, in the case of $\tau_2^{(2)} > \tau_{\max}$ a naive interpretation of experimental data shows, for $K_2(\tau)$, a power-law decay like $\tau^{-2\alpha}$, which corresponds to the memory exponent $\alpha^* = \alpha + 0.5$. The genuine memory exponent α appears only in the time scale $\tau \gg \tau_2^{(2)}$. From Eqs. (A24) and (A25) there follows a somewhat surprising circumstance that in crossover regions the pictures of the asymptotic dependence of $K_1(\tau)$ and $K_2(\tau)$ on τ are different. First, although in the long-time-lag regime both of the normalized cross-correlation functions $K_1(\tau)$ and $K_2(\tau)$ decay similarly as $\tau^{-(2\alpha-1)}$, below the characteristic crossover time $\tau_2^{(i)}$ the functions $K_1(\tau)$ and $K_2(\tau)$ relax asymptotically as $\tau^{-\alpha}$ and $\tau^{-2\alpha}$, respectively. Thus in this region $K_2(\tau)$ exhibits a much faster decay than $K_1(\tau)$ (see. Fig. 5). Second, for physically reasonable values of the friction coefficient, $\gamma/\omega^{2-\alpha} < 10$, the crossover time $\tau_2^{(1)}$ for $K_1(\tau)$ is always significantly larger than $\tau_2^{(2)}$ for $K_2(\tau)$ [cf. Eqs. (50) and (51)]. We emphasize that the above described crossover effects occur only in the presence of multiplicative noise. Since without multiplicative noise such effects are absent, the appearance of power-law regimes with different exponents for $K_1(\tau)$ and $K_2(\tau)$ in possible microrheology experiments is an indication of the presence of a multiplicative noise influencing the dynamics of the system. It should be noted that a similar phenomenon of a multiplicative-noise-induced crossover between two different asymptotic power-law regimes for correlation functions have been previously considered for a fractional oscillator in Ref. [36].

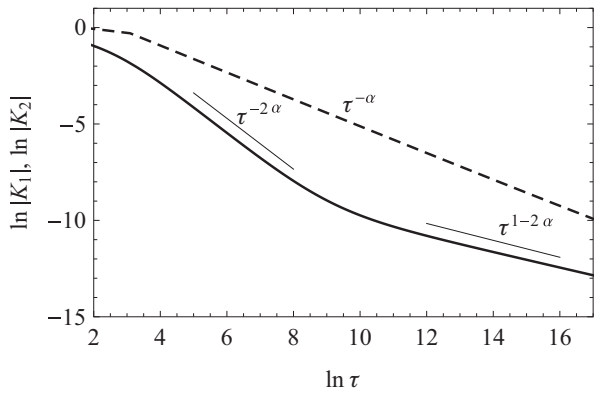

FIG. 5. A logarithmic plot of the asymptotic dependence of the normalized cross-correlation functions $K_1(\tau)$ and $K_2(\tau)$ on the time lag τ. System parameter values: $\gamma = 4$, $\rho = k_BT = \omega = 1$, $\Omega = 0$, $\alpha = 0.7$, and $D = 5.7897$. Solid line, $\ln|K_2(\tau)|$ vs $\ln\tau$; dashed line $\ln|K_1(\tau)|$ vs $\ln\tau$. Note a crossover between two asymptotic power-law regimes, $\tau^{-1.4}$ and $\tau^{-0.4}$, at the characteristic lag-time value $\ln\tau_2^{(2)} = 8.9872$.

B. Oscillatory shear flow

In Eq. (3) the shear flow ($\Omega \neq 0$) can be considered as an external periodic driving force. As such, it allows excitation of internal modes of the unperturbed system [30]. We now explicitly consider the spatial moments and particle angular momentum, where resonance effects manifest themselves as amplitude peaks at particular shear frequencies Ω. Since the component Y is not affected by the shear flow, its second moment $\langle Y^2\rangle_{as}$ is a constant, Eq. (26). To discern memory effects from those generated by multiplicative noise we now consider the case without multiplicative noise, $D = 0$. The dependence of the amplitude $|B_1|$ for the time-dependent contribution to $\langle X^2(t)\rangle_{as}$ [cf. Eq. (36)] on the frequency Ω is shown in Fig. 6(a) for different values of the memory exponent α. These graphs show a typical multiresonance, with nonmonotonic behavior for the frequencies Ω close to several resonance frequencies, which is a bona fide resonance phenomenon. For intermediate values of the memory exponent α, but relatively low values of the friction coefficient γ the amplitude $|B_1|$ exhibits three resonance peaks at $\Omega \approx 0.5\omega$, $\Omega \approx \omega$, and $\Omega \approx 2\omega$. As a rule the peak near the trap frequency, $\Omega \approx \omega$, becomes the dominant resonance at intermediate values of $\gamma < \omega^{2-\alpha}$. The peaks at ω and 2ω are connected with the resonant behavior of the cross-moment $\langle X(t)Y(t)\rangle_{as}$. Namely, from Eqs. (29) and (32) it follows that the amplitude $|A(\infty)|$ exhibits resonances near $\Omega \approx 2\omega$ and $\Omega = \omega$, which

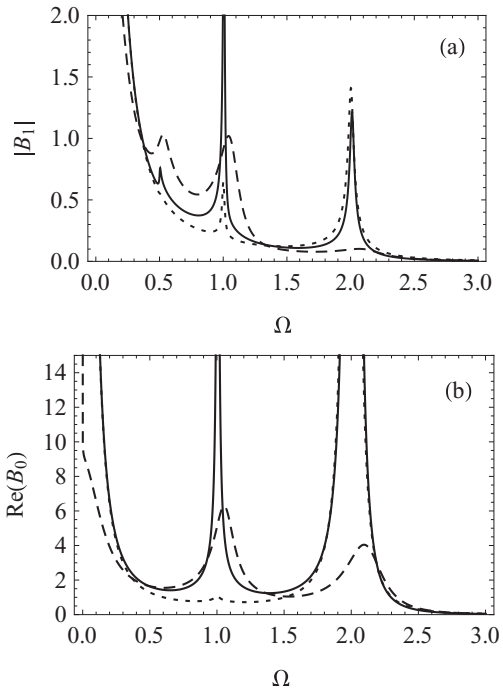

FIG. 6. Multiresonance of the second moment $\langle X^2\rangle_{as}$ characteristics $\mathrm{Re}(B_0)$ and $|B_1|$ [see Eq. (36)] computed from Eq. (A16) at $\omega = 1$, and $D = 0$. (a) depicts the resonancelike behavior of the amplitude $|B_1|$ for the time-dependent contribution to $\langle X^2\rangle_{as}$ vs the frequency Ω of the shear flow. (b) Dependence of the time-independent quantity $\mathrm{Re}(B_0)$ in Eq. (36) on Ω. Solid lines: $\alpha = 0.6$ and $\gamma = 0.02$; dashed lines: $\alpha = 0.6$ and $\gamma = 0.2$; dotted lines: $\alpha = 0.9$; $\gamma = 0.02$. The values of $\mathrm{Re}(B_0)$ and $|B_1|$ at the local maxima: solid lines, $\mathrm{Re}[B_0(1)] \approx 39.93$, $\mathrm{Re}[B_0(2)] \approx 476.78$, and $|B_1(1)| \approx 2.86$; dotted line, $\mathrm{Re}[B_0(2)] \approx 318.87$. More details in the text.

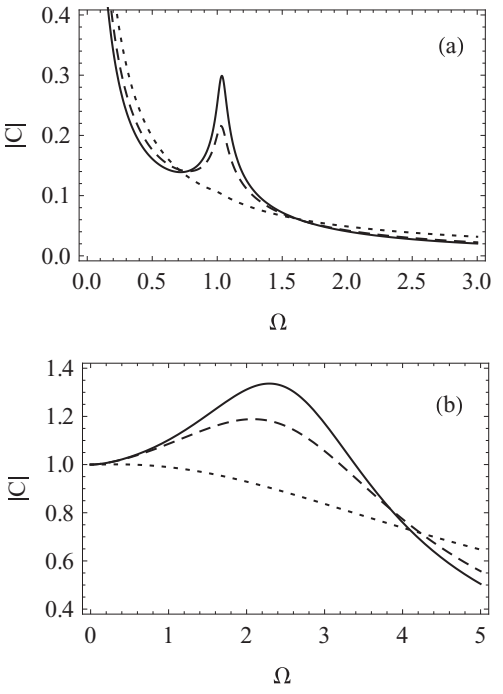

FIG. 7. Resonance for the particle angular momentum $\langle L_z\rangle_{as}$ versus the shear flow frequency Ω at different values of the memory exponent α, [cf. Eq. (42)]. The amplitude $|C|$ of $\langle L_z\rangle_{as}$ is computed from Eq. (A13) with $\omega = 1$ and $D = 0$. Solid lines, $\alpha = 0.5$; dashed lines, $\alpha = 0.6$; dotted lines, $\alpha = 0.95$. At high values of the shear flow frequency, $\Omega \to \infty$, the amplitude $|C|$ tends to 0. In the limit of zero frequency, $\Omega \to 0$, the value of $|C|$ approaches 1. (a) $\gamma = 0.1$, (b) $\gamma = 4.3$. More details in the text.

become less pronounced as γ increases. The resonance for $|B_1|$ at $\Omega \approx 2\omega$ is dominant for low values of the friction coefficient, $\gamma \ll \omega^{2-\alpha}$. The third peak at $\Omega \approx 0.5\omega$ is relatively small and decreases as the memory exponent α increases. The time-independent term $\mathrm{Re}(B_0)$ in Eq. (36) has a two-peak structure by $\gamma < \omega^{2-\alpha}$ [cf. Fig. 6(b)]. The resonances appear at the frequencies $\Omega \approx 2\omega$ and $\Omega \approx \omega$. Although the peak at $\Omega \approx 2\omega$ tends to dominate, at sufficiently small values of the memory exponent α (near the subdiffusive regime of $\langle X^2\rangle$) the peak at $\Omega \approx \omega$ can become the dominant resonance. The resonances of $\langle X^2(t)\rangle_{as}$ vs Ω disappear at sufficiently large values of the friction coefficient, $\gamma > \omega^{2-\alpha}$. It should be noted that both the term $\mathrm{Re}(B_0)$ and the amplitude $|B_1|$ attain large values near $\Omega = 0$ (a finite value for $\alpha > 2/3$; unlimited growth for $0.5 < \alpha \leqslant 2/3$) and vanish in the limit $\Omega \to \infty$. In the last case the particles are too inert to adjust to the motion of the flow. Before we study the resonance of the particle angular momentum $\langle L_z(t)\rangle_{as}$, Eq. (42), we compare our results with the case of Stokes friction, which have been previously calculated in Ref. [30]. By taking the limit $\alpha \to 1$ in Eqs. (3) and (4) we see that the noise $\boldsymbol{\xi}(t)$ corresponds to white noise and, consequently, to Stokes friction. In this limit the quantities $\mathrm{Re}(B_0)$ and $|B_1|$ are characterized with one resonance peak at $\Omega \approx 2\omega$ and two peaks at $\Omega \approx \omega$ and $\Omega \approx 2\omega$, respectively. Thus, in some cases the number and location of the resonance peaks of $\langle X^2(t)\rangle_{as}$ vs Ω can give an indicator to estimate the viscoelastic properties of the medium in experiments such as described in Ref. [30].

Our next task is to examine the dependence of the amplitude C of $\langle L_z(t)\rangle_{as}$, Eq. (42), on the shear flow frequency Ω. In the case of Stokes friction, $\alpha = 1$, it follows from Eq. (43) that

$$|C| = \left[1 + \left(\frac{\Omega}{\gamma}\right)^2\right]^{-\frac{1}{2}}; \tag{52}$$

consequently $|C(\Omega)|$ decreases monotonically as Ω increases (cf. also Ref. [30]). If the shear flow is viscoelastic, $\alpha < 1$, the behavior of $|C(\Omega)|$ is more complicated. The results for the particle angular momentum are illustrated in Fig. 7. For weak friction, $\gamma < \omega^{2-\alpha}$, the amplitude $|C(\Omega)|$ exhibits a clear resonance at $\Omega \approx \omega$, which becomes less pronounced as the memory exponent α increases. The resonance effect becomes much less obvious at intermediate values of the friction coefficient, $\gamma \approx \omega^{2-\alpha}$, and at $\alpha \approx 1$, where the resonance is suppressed. It is important to note that in the case of strong friction, $\gamma > \omega^{2-\alpha}$, the resonance also occurs, but the location of the resonance peak is significantly shifted from the trap frequency ω to greater values of Ω, which tends to the value 2ω as α decreases. Here we emphasize that in this case the value of $|C|$ increases at resonance maxima by increasing the friction coefficient γ and is larger than in the low-frequency limit, $|C| > |C(0)| = 1$. As mentioned above, the resonance disappears at sufficiently large values of the memory exponent, $\alpha \approx 1$, particularly in the case of Stokes friction. Thus we have

found an experimentally convenient criterion that enables us to verify the importance of viscoelasticity in shear flow as a factor of the dynamics of Brownian particles.

IV. CONCLUSIONS

We have studied, in the long-time regime, the dynamics of an underdamped Brownian particle in a fluctuating trapping potential well, which is simultaneously subjected to an oscillatory viscoelastic shear flow. Starting from a generalized Langevin equation with a power-law-type memory driven by an internal noise and a multiplicative noise [Eq. (3)], we have been able to derive exact analytical expressions of the second-order moments and cross-correlation functions of the fluctuating displacement for the Brownian particle in the shear plane.

As our main result we have established that in the investigated model an interplay of the multiplicative noise, the shear flow, and memory effects can generate a rich variety of nonequilibrium cooperation phenomena. Namely, (i) the existence of critical memory exponents $\alpha_{cr1} = \frac{1}{2}$ and $\alpha_{cr2} = \frac{2}{3}$ for oscillatory and time-independent shear flows, respectively, which mark dynamical transitions from the confined dynamics of a Brownian particle to the subdiffusive regime; (ii) a resonancelike dependence of the anisotropy of the particle position distribution on the memory exponent α; (iii) a crossover between two different asymptotic power-law regimes in time τ for the cross-correlation functions, e.g., $\tau^{-2\alpha}$ and $\tau^{1-2\alpha}$ for $\langle X(t)Y(t+\tau)\rangle_{as}$; (iv) multiresonance of the second moment of the particle displacement in the shear flow direction $\langle X^2\rangle$ and the cross-correlation $\langle XY\rangle$ between the orthogonal directions in the shear plane versus the frequency Ω of the shear flow (up to three peaks for $\langle X^2\rangle$ and up to two peaks for $\langle XY\rangle$); (v) the existence of a memory-dependent critical intensity of the fluctuations of the trapping potential well, above which an energetic instability occurs; (vi) resonance of the mean angular momentum $\langle L_z\rangle$ of Brownian particles versus the frequency Ω. The last effect, i.e., the resonance of $\langle L_z\rangle$ vs Ω, is relatively strong at intermediate values of the memory exponent α. This contrasts with the case of Stokes friction ($\alpha = 1$) in the shear flow, where such an effect is absent (the amplitude of $\langle L_z\rangle$ is a decreasing function on Ω, [30]). Thus it seems that the appearance of a resonant peak of $\langle L_z\rangle$ vs Ω can provide an experimentally convenient criterion enabling estimation of the importance of the viscoelastic properties of the shear flow.

We believe that the results of this paper not only supply material for theoretical investigations of fractional dynamics in stochastic systems, but also suggest some possibilities for interpreting experimental data, e.g., for particles trapped by optical tweezers in dusty plasmas and in the cytoplasm of cells, where issues of memory and multiplicative noise can be crucial [20,21,41]. A possible perspective is to apply our results in the design of experiments with optical tweezers, such as employed in Ref. [40] for direct measurements of the Brownian motion of micron-sized beads in a shear flow. For an oscillatory shear flow possible experiments on dusty plasmas and trapped colloidal dispersions have been discussed in Ref. [30].

Finally, according to the results of Ref. [30] for Stokes friction, we speculate that the model discussed in this paper can be expanded, along the lines described in Ref. [30], to one suitable for studying interacting many-particle systems.

ACKNOWLEDGMENTS

The work was supported by the Estonian Science Foundation under Grant No. 9005, by the Ministry of Education and Research of Estonia under Grant No. SF0130010s12, by the International Atomic Energy Agency under Grant No. 14797, and by the European Union trough the European Regional Development Fund (Centre of Excellence "Mesosystems: Theory and Applications", TK 114).

APPENDIX A: FORMULAS FOR THE RELAXATION FUNCTIONS

1. Time dependence of the relaxation functions $H(t)$ and $G(t)$

The relaxation functions $H(t)$ and $G(t)$ in Eqs. (17) and (18) can be obtained by means of the Laplace transformation technique. To evaluate the inverse Laplace transform of $\hat{G}(s)$ and $\hat{H}(s)$ [see Eqs. (19) and (20)] we use the residue theorem method described in Ref. [42]. The inverse Laplace transform gives

$$H(t) = \frac{\gamma \sin(\alpha\pi)}{\pi}\int_0^\infty \frac{r^\alpha e^{-rt}dr}{B(r)} + \frac{2}{\sqrt{u^2+v^2}}\mathrm{Im}[e^{i\Theta}e^{-(\beta-i\omega^*)t}], \tag{A1}$$

$$G(t) = \frac{\omega^2\gamma \sin(\alpha\pi)}{\pi}\int_0^\infty \frac{e^{-rt}dr}{r^{1-\alpha}B(r)} + \frac{2\omega^2}{\sqrt{u^2+v^2}}\mathrm{Im}\left[\frac{e^{i\Theta}e^{-(\beta-i\omega^*)t}}{\beta-i\omega^*}\right]. \tag{A2}$$

Here $s_{1,2} = -\beta \pm i\omega^*$, ($\beta > 0, \omega^* > 0$) are the pair of conjugate complex zeros of the equation

$$s^2 + \gamma s^\alpha + \omega^2 = 0, \tag{A3}$$

where Eq. (A3) is defined by the principal branch of s^α. The quantities u, v, Θ, and $B(r)$ are determined by

$$u = -2\beta + \frac{\gamma\alpha\cos[(1-\alpha)\varphi]}{(\beta^2+\omega^{*2})^{\frac{1-\alpha}{2}}}, \tag{A4}$$

$$v = 2\omega^* - \frac{\gamma\alpha\sin[(1-\alpha)\varphi]}{(\beta^2+\omega^{*2})^{\frac{1-\alpha}{2}}}, \tag{A5}$$

with

$$\varphi = \pi + \arctan\left(-\frac{\omega^*}{\beta}\right), \tag{A6}$$

$$\Theta = \arctan\left(\frac{u}{v}\right), \tag{A7}$$

and

$$B(r) := [r^2 + \gamma r^\alpha\cos(\pi\alpha) + \omega^2]^2 + \gamma^2 r^{2\alpha}\sin^2(\alpha\pi). \tag{A8}$$

The relaxation functions $H(t)$ and $G(t)$ can be represented via Mittag-Leffler-type special functions [33]. But as in the last case the numerical calculations are very complicated, so we suggest, apart from possible representations via Mittag-Leffler functions, a numerical treatment of Eqs. (A1) and (A2). It should be noted that the representations (A1) and (A2) for the relaxation functions $H(t)$ and $G(t)$ have been previously used by analysis of the energetic stability and temporal behavior

of the autocorrelation functions of a fractional oscillator with multiplicative noise [36,37].

2. Integrals for relaxation functions

Here the exact formulas for the quantities $\psi(t)$, $\phi(\Omega)$, $A(\infty)$, C, and B_j, which determine the long-time behavior of the second moments, are presented. From Eqs. (27), (38), and (A1) one can conclude that the $\psi(t)$ and $\phi(\Omega)$ are given by

$$\psi(t) = \frac{\gamma \sin(\alpha\pi)}{\pi}\int_0^\infty \frac{r^\alpha e^{-rt}}{B(r)}\hat{H}(r)dr + \frac{2e^{-\beta t}}{\sqrt{u^2+v^2}}\mathrm{Im}[e^{i(\omega^* t+\Theta)}\hat{H}(\beta - i\omega^*)] \quad \text{(A9)}$$

and

$$\phi(\Omega) = \frac{\gamma \sin(\alpha\pi)}{\pi}\int_0^\infty \frac{r^\alpha}{B(r)}\hat{H}(r-2i\Omega)dr + \frac{1}{i\sqrt{u^2+v^2}}\{e^{i\Theta}\hat{H}[\beta - i(\omega^*+2\Omega)] - e^{-i\Theta}\hat{H}[\beta + i(\omega^*-2\Omega)]\}, \quad \text{(A10)}$$

where

$$\hat{H}(s) = \frac{1}{s^2+\gamma s^\alpha+\omega^2}. \quad \text{(A11)}$$

Using formulas (30), (31), (A1), and (A9) we obtain, for complex amplitudes $A(\infty)$ and C of the cross correlation $\langle XY\rangle$ and of the angular momentum $\langle L_z\rangle$ [see Eqs. (33) and (43)], respectively:

$$A(\infty) = \frac{\gamma \sin(\alpha\pi)}{\pi}\int_0^\infty \frac{r^\alpha f(r)}{B(r)}\hat{\chi}(r+i\Omega)dr + \frac{1}{i\sqrt{u^2+v^2}}\{e^{i\Theta}f(\beta - i\omega^*)\hat{\chi}[\beta - i(\omega^*-\Omega)] - e^{-i\Theta}f(\beta+i\omega^*)\hat{\chi}[\beta+i(\omega^*+\Omega)]\} \quad \text{(A12)}$$

and

$$C = \frac{\gamma^2 \sin(\alpha\pi)}{\pi}\int_0^\infty \frac{r^\alpha f(r)(2r+i\Omega)}{B(r)}\hat{\chi}(r+i\Omega)dr + \frac{\gamma}{i\sqrt{u^2+v^2}}\{e^{i\Theta}f(\beta - i\omega^*)[2\beta - i(2\omega^*-\Omega)] \times \hat{\chi}[\beta - i(\omega^*-\Omega)] - e^{-i\Theta}f(\beta+i\omega^*)[2\beta+i(2\omega^*+\Omega)]\hat{\chi}[\beta+i(\omega^*+\Omega)]\}, \quad \text{(A13)}$$

where

$$f(s) := 2D\hat{H}(s) + \frac{\omega^2}{s}[1-2D\psi(0)], \quad \text{(A14)}$$

$$\hat{\chi}(s) = \frac{s^{\alpha-1}}{s^2+\gamma s^\alpha+\omega^2}. \quad \text{(A15)}$$

For the second moment $\langle X^2(t)\rangle$ [see Eq. (36)] the integrals B_j, $j = 0,1$, can be evaluated as follows:

$$B_j = \frac{\sin(\alpha\pi)}{\pi}\int_0^\infty \frac{(\omega^2+r^2)}{r^{1-\alpha}B(r)}\hat{\chi}(r+i\Omega 2j)\hat{F}[r+i\Omega(2j-1)]dr + \frac{1}{i\sqrt{u^2+v^2}} \times \left\{\frac{e^{i\Theta}}{(-\beta+i\omega^*)^{1-\alpha}}\hat{\chi}[\beta - i(\omega^*-2j\Omega)]\hat{F}\{\beta - i[\omega^*-(2j-1)\Omega]\} - \frac{e^{-i\Theta}}{(-\beta-i\omega^*)^{1-\alpha}}\hat{\chi}[\beta+i(\omega^*+2j\Omega)]\hat{F}\{\beta+i[\omega^*+(2j-1)\Omega]\}\right\}, \quad \text{(A16)}$$

where

$$\hat{F}(s) = \frac{\gamma \sin(\alpha\pi)}{\pi}\int_0^\infty \frac{r^\alpha f(r)dr}{(r+s)B(r)} + \frac{1}{i\sqrt{u^2+v^2}} \times \left[\frac{e^{i\Theta}f(\beta - i\omega^*)}{\beta+s-i\omega^*} - \frac{e^{-i\Theta}f(\beta+i\omega^*)}{\beta+s+i\omega^*}\right]. \quad \text{(A17)}$$

3. Asymptotic behavior of relaxation functions

The asymptotic behavior of the relaxation functions $H(t)$, $G(t)$, and $\psi(t)$ at large t has been previously considered in Ref. [36]. From Eqs. (A1), (A2), and (A9) it follows that in a long-time limit ($t \to \infty$), these functions decay as a power law

$$H(t) \sim \frac{\gamma\alpha}{\omega^4\Gamma(1-\alpha)}t^{-(1+\alpha)}, \quad \text{(A18)}$$

$$G(t) \sim \frac{\gamma}{\omega^2\Gamma(1-\alpha)}t^{-\alpha}, \quad \text{(A19)}$$

$$\psi(t) \sim \frac{\gamma\alpha}{\omega^6\Gamma(1-\alpha)}t^{-(1+\alpha)}. \quad \text{(A20)}$$

Using Eqs. (30) and (31) we see that

$$F(t) \sim G(t)[1-2D\psi(0)], \quad \chi(t) \sim \frac{1}{\gamma}G(t) \quad \text{(A21)}$$

at $t \to \infty$. The asymptotic formulas (A19) and (A21) are used for estimation of the behavior of second moments in nonstationary regimes (Sec. II C).

4. Asymptotic behavior of cross-correlation functions

As shown experimentally in Ref. [40], the shear induced asymmetry of cross-correlation functions $\langle X(t+\tau)Y(t)\rangle \neq \langle X(t)Y(t+\tau)\rangle$ with respect to the time lag τ is one of the important effects of shear flow on the distribution of particle fluctuations. In the case of a stationary regime of the model (3) these functions can be expressed as [see also Eqs. (30), (31), (A1), (A2), and (A9)]

$$\langle Y(t+\tau)X(t)\rangle_{as} = \gamma\rho\langle Y^2\rangle_{as}\mathrm{Re}\left[e^{i\Omega t}\int_0^\infty e^{-i\Omega t_1}\chi(t_1)F(t_1+\tau)dt_1\right] \quad \text{(A22)}$$

and

$$\langle Y(t)X(t+\tau)\rangle_{as} = \gamma\rho\langle Y^2\rangle_{as}\mathrm{Re}\left\{e^{i\Omega t}\left[\int_0^\infty dt_1 e^{-i\Omega t_1}F(t_1)\chi(t_1+\tau) + \int_0^\tau dt_1 e^{i\Omega t_1}\chi(\tau-t_1)F(t_1)\right]\right\}. \quad \text{(A23)}$$

If $\Omega \neq 0$, then the formulas (A22) and (A23) are applicable for all values of the memory exponent, $0<\alpha<1$, but for $\Omega = 0$, a stationary regime is possible only if $1/2<\alpha<1$.

From Eqs. (A22) and (A23) it follows that for large τ the cross-correlation functions decay as a power law. Namely, at a long-time limit ($\tau\to\infty$), the asymptotic behavior of $\langle Y(t+\tau)X(t)\rangle_{as}$ and $\langle Y(t)X(t+\tau)\rangle_{as}$ for $\Omega = 0$ and $1/2<\alpha<1$ reads as:

$$\langle Y(t+\tau)X(t)\rangle_{as} \sim \rho\langle Y^2\rangle_{as}\frac{\gamma^2\sin(\alpha\pi)}{\pi\omega^6}\left\{\frac{2D}{\omega^2}\cdot\frac{\Gamma(2\alpha)}{\tau^{2\alpha}} + \omega^2[1-2D\psi(0)]\frac{\Gamma(2\alpha-1)}{\tau^{2\alpha-1}}\right\}, \quad \text{(A24)}$$

$$\langle X(t+\tau)Y(t)\rangle_{as} \sim \rho\gamma^2\langle Y^2\rangle_{as}\frac{\sin(\alpha\pi)}{\pi\omega^6}\left[\frac{2D\Gamma(\alpha)}{\gamma\tau^\alpha} + \omega^2[1-2D\psi(0)] \times [1-2\cos(\alpha\pi)]\frac{\Gamma(2\alpha-1)}{\tau^{2\alpha-1}}\right]. \quad \text{(A25)}$$

APPENDIX B: PRINCIPAL AXES OF THE COVARIANCE MATRIX

In the stationary regime the particles positional distribution in an x-y plane is characterized with the covariance matrix (see Ref. [23])

$$\boldsymbol{M} = \begin{pmatrix}\langle X^2\rangle_{as} & \langle XY\rangle_{as}\\ \langle XY\rangle_{as} & \langle Y^2\rangle_{as}\end{pmatrix}. \quad \text{(B1)}$$

According to Ref. [23] the lengths of the principal axes $C_{1,2}$ of the elliptical distributions are given by the eigenvalues $C_{1,2}^2$ of the matrix $\boldsymbol{M}$

$$C_{1,2}^2 = \tfrac{1}{2}[\langle X^2\rangle_{as}+\langle Y^2\rangle_{as}] \pm \tfrac{1}{2}\sqrt{4\langle XY\rangle_{as}^2+[\langle X^2\rangle_{as}-\langle Y^2\rangle_{as}]^2}, \quad \text{(B2)}$$

where the subscript 1 (2) refers to the plus (minus) sign. The longer axis is rotated counterclockwise with respect to the x axis by an angle ϕ, which is given by the expression

$$\tan\phi = \frac{\langle XY\rangle_{as}}{C_1^2-\langle Y^2\rangle_{as}}. \quad \text{(B3)}$$

APPENDIX C: PROOF OF EQS. (14) AND (40)

For the sake of simplicity, here we restrict ourselves to a special type of white noise $Z_i(t)$, which can be considered as a limit process of the Markovian telegraph noise (dichotomous noise) $\widetilde{Z}(t)$ with a zero mean and exponential correlator

$$\langle\widetilde{Z}(t)\rangle = 0, \quad \langle\widetilde{Z}(t_1)\widetilde{Z}(t_2)\rangle = a^2e^{-\nu|t_2-t_1|}, \quad \text{(C1)}$$

where the random variable $\widetilde{Z}(t)$ takes the values $\widetilde{Z}=\pm a$, so that $[\widetilde{Z}(t)]^2 = a^2$, with the mean waiting time $(\nu/2)^{-1}$ in both states [43]. Transition to white noise occurs if $\nu\to\infty$, $a^2\to\infty$, so that a^2/ν equals a finite constant D (the intensity of the white noise) [43,44]. As was shown in Ref. [43], the correlation function and higher-order moment functions at such a limit process are the same as for a δ-correlated process with the properties (7).

Assuming that the noise $\widetilde{\boldsymbol{Z}}(t) = [\widetilde{Z}_1(t),\widetilde{Z}_2(t),\widetilde{Z}_3(t)]$ is statistically independent from the noise $\boldsymbol{\xi}(t)$ [$\widetilde{Z}_i(t)$ are statistically independent dichotomous noises with properties (C1)] and replacing now Z_2 in Eq. (9) with $\widetilde{Z}$, it can be rewritten as two differential equations:

$$\dot{Y}(t) = p(t), \quad \text{(C2)}$$

$$\dot{p}(t) = -\gamma\frac{d^\alpha}{dt^\alpha}Y(t) - [\omega^2+\widetilde{Z}(t)]Y(t)+\xi_2(t). \quad \text{(C3)}$$

Multiplying Eqs. (C2) and (C3) by $\widetilde{Z}(t)$ one gets (after averaging over an ensemble of realizations of the multiplicative noise)

$$\langle\widetilde{Z}Y\rangle_Z^{\cdot} = -\nu\langle\widetilde{Z}Y\rangle_Z + \langle\widetilde{Z}p\rangle_Z, \quad \text{(C4)}$$

$$\langle\widetilde{Z}p\rangle_Z^{\cdot} = -\nu\langle\widetilde{Z}p\rangle_Z - \frac{\gamma}{\Gamma(1-\alpha)}\int_0^t\frac{e^{-\nu(t-t')}}{(t-t')^\alpha} \times\langle\widetilde{Z}(t')p(t')\rangle_Z dt' - \omega^2\langle\widetilde{Z}Y\rangle_Z - a^2\langle Y\rangle_Z. \quad \text{(C5)}$$

Here we have used the Shapiro-Loginov formula for the dichotomous noise $\widetilde{Z}(t)$

$$\langle\widetilde{Z}(t)\phi_t(\widetilde{Z})\rangle_Z^{\cdot} = \langle\widetilde{Z}(t)\frac{d}{dt}\phi_t(\widetilde{Z})\rangle_Z - \nu\langle\widetilde{Z}(t)\phi_t(\widetilde{Z})\rangle_Z, \quad \text{(C6)}$$

where $\phi_t(\widetilde{Z})$ is an arbitrary functional of $\widetilde{Z}(t')$ involving only times $t'\leqslant t$ [45], and the equality (see also Refs. [43,46])

$$\langle\widetilde{Z}(t)\phi_{t'}(\widetilde{Z})\rangle_Z = \frac{1}{a^2}\langle\widetilde{Z}(t)\widetilde{Z}(t')\widetilde{Z}(t')\phi_{t'}(\widetilde{Z})\rangle_Z = e^{-\nu(t-t')}\langle\widetilde{Z}(t')\phi_{t'}(\widetilde{Z})\rangle_Z, \quad t'\leqslant t. \quad \text{(C7)}$$

Assuming that the correlators $\langle\widetilde{Z}Y\rangle_Z$ and $\langle\widetilde{Z}p\rangle_Z$ are bounded, we obtain after the limit procedure ($\nu\to\infty$, $a^2\to\infty$, $a^2/\nu = D$):

$$\langle Z_2Y\rangle_Z = 0, \quad \langle Z_2\dot{Y}\rangle_Z = -D\langle Y\rangle_Z. \quad \text{(C8)}$$

Analogously, using that in Eq. (10) Y is independent of noise Z_1 one gets

$$\langle Z_1 X\rangle_Z = 0, \quad \langle Z_1 \dot{X}\rangle_Z = -D\langle X\rangle_Z. \tag{C9}$$

Thus, we have verified Eq. (14) for fractional dynamics described by Eqs. (3)–(7).

The results (C8) and (C9) are not restricted to the special type of white noise with the condition represented in Eq. (7) for higher-order moment functions. For example, considering that the random process

$$\widetilde{\widetilde{Z}}_N(t) = \widetilde{Z}_1(t) + \cdots + \widetilde{Z}_N(t),$$

where $\widetilde{Z}_k(t)$ are statistically independent processes with the properties of $\widetilde{Z}(t)$ with $\widetilde{Z}^2 = a^2/N$, we obtain that the process $\widetilde{\widetilde{Z}}(t) = \lim_{N\to\infty} \widetilde{\widetilde{Z}}_N(t)$ is a Gaussian Markovian process [43]. Thus, Eqs. (C8) and (C9) are valid also in the case of the Gaussian white noise $Z_i(t)$.

To derive Eq. (40) we emphasize that due to statistical independence of the noises $\widetilde{\boldsymbol{Z}}(t)$ and $\boldsymbol{\xi}(t)$

$$\langle \boldsymbol{\xi}(t_1)\widetilde{\boldsymbol{Z}}(t_2)\widetilde{X}(t_2)\rangle = \langle \boldsymbol{\xi}(t_1)\langle \widetilde{\boldsymbol{Z}}(t_2)\widetilde{X}(t_2)\rangle_Z\rangle_\xi, \tag{C10}$$

where $\langle\rangle_\xi$ denotes an average over an ensemble of realizations of the random process $\boldsymbol{\xi}(t)$ and $\widetilde{X}(t)$ is determined with Eq. (10), where the noise $\boldsymbol{Z}(t)$ is replaced with the dichotomous noise $\widetilde{\boldsymbol{Z}}(t)$. As the process $\boldsymbol{\xi}(t)$ is independent from the dichotomous noise parameters a and ν the limit procedure ($\nu\to\infty, a^2\to\infty, a^2/\nu = D$) gives

$$\begin{aligned}\langle \boldsymbol{\xi}(t_1)\boldsymbol{Z}(t_2)X(t_2)\rangle &= \langle \boldsymbol{\xi}(t_1)\langle \boldsymbol{Z}(t_2)X(t_2)\rangle_Z\rangle_\xi \\ &= \langle \boldsymbol{\xi}(t_1)\times 0\rangle = 0,\end{aligned}$$

where we have used Eqs. (C8) and (C9) and the equality

$$\begin{aligned}&\left\langle \widetilde{Z}_2(t)\frac{d^\alpha}{dt^\alpha}\left[\int_0^t Y(t')\cos(\Omega t')dt'\right]\right\rangle_Z \\ &= e^{-\nu t}\frac{d^\alpha}{dt^\alpha}\left[\int_0^t e^{\nu t'}\langle \widetilde{Z}_2(t')Y(t')\rangle_Z\cos(\Omega t')dt'\right].\end{aligned}$$

Thus, we have verified Eq. (40).

Finally, we note that the equation of motion of the ordinary oscillator with a random frequency has been studied extensively. It turns out that fluctuations of the frequency do not affect the first moment of the underdamped oscillator provided the fluctuations are δ-correlated (see, e.g., Refs. [35,43,44,46]). This fact is in accordance with Eq. (14) with $\alpha = 1$.

[1] L. Gammaitoni, P. Hänggi, P. Jung, and F. Marchesoni, Rev. Mod. Phys. **70**, 223 (1998).
[2] R. Mankin, K. Laas, T. Laas, and E. Reiter, Phys. Rev. E **78**, 031120 (2008).
[3] R. A. Ibrahim, J. Vib. Control **12**, 1093 (2006).
[4] R. Mankin, E. Soika, A. Sauga, and A. Ainsaar, Phys. Rev. E **77**, 051113 (2008).
[5] S. L. Ginzburg and M. A. Pustovoit, Phys. Rev. Lett. **80**, 4840 (1998).
[6] R. Mankin, A. Haljas, R. Tammelo, and D. Martila, Phys. Rev. E **68**, 011105 (2003).
[7] M. O. Magnasco, Phys. Rev. Lett. **71**, 1477 (1993).
[8] P. Reimann, Phys. Rep. **361**, 57 (2002).
[9] W. Götze and L. Sjögren, Rep. Prog. Phys. **55**, 241 (1992).
[10] T. Carlsson, L. Sjögren, E. Mamontov, and K. Psiuk-Maksymowicz, Phys. Rev. E **75**, 031109 (2007).
[11] S. C. Weber, A. J. Spakowitz, and J. A. Theriot, Phys. Rev. Lett. **104**, 238102 (2010).
[12] Q. Gu, E. A. Schiff, S. Grebner, F. Wang, and R. Schwarz, Phys. Rev. Lett. **76**, 3196 (1996).
[13] S. C. Kou and X. S. Xie, Phys. Rev. Lett. **93**, 180603 (2004).
[14] W. Min, G. Luo, B. J. Cherayil, S. C. Kou, and X. S. Xie, Phys. Rev. Lett. **94**, 198302 (2005).
[15] J. M. Porrá, K.-G. Wang, and J. Masoliver, Phys. Rev. E **53**, 5872 (1996).
[16] E. Lutz, Phys. Rev. E **64**, 051106 (2001).
[17] S. Burov and E. Barkai, Phys. Rev. E **78**, 031112 (2008).
[18] S. Warlus and A. Ponton, Rheol. Acta **48**, 51 (2009).
[19] I. Goychuk, Phys. Rev. E **80**, 046125 (2009).
[20] I. M. Tolić-Nørrelykke, E.-L. Munteanu, G. Thon, L. Oddershede, and K. Berg-Sørensen, Phys. Rev. Lett. **93**, 078102 (2004).
[21] R. Granek and J. Klafter, Phys. Rev. Lett. **95**, 098106 (2005).
[22] R. Kubo, Rep. Prog. Phys. **29**, 255 (1966).
[23] L. Holzer, J. Bammert, R. Rzehak, and W. Zimmermann, Phys. Rev. E **81**, 041124 (2010).
[24] B. Lander, U. Seifert, and T. Speck, Phys. Rev. E **85**, 021103 (2012).
[25] A. Groisman and V. Steinberg, Nature (London) **410**, 905 (2001).
[26] T. T. Perkins, D. E. Smith, and S. Chu, Science **276**, 2016 (1997).
[27] A. Groisman and V. Steinberg, Nature (London) **405**, 53 (2000).
[28] R. Rzehak and W. Zimmermann, Physica A **324**, 495 (2003).
[29] J. Bammert and W. Zimmermann, Phys. Rev. E **82**, 052102 (2010).
[30] H. Kählert and H. Löwen, Phys. Rev. E **86**, 041119 (2012).
[31] T. A. Waigh, Rep. Prog. Phys. **68**, 685 (2005).
[32] Y. Roichman, B. Sun, A. Stolarski, and D. G. Grier, Phys. Rev. Lett. **101**, 128301 (2008).
[33] I. Podlubny, *Fractional Differential Equations* (Academic Press, San Diego, 1999).
[34] E. Soika, R. Mankin, and A. Ainsaar, Phys. Rev. E **81**, 011141 (2010).
[35] K. Lindenberg, V. Seshadri, and B. J. West, Phys. Rev. A **22**, 2171 (1980).
[36] R. Mankin, K. Laas, and A. Sauga, Phys. Rev. E **83**, 061131 (2011).
[37] R. Mankin and A. Rekker, Phys. Rev. E **81**, 041122 (2010).
[38] L. Bruno, V. Levi, M. Brunstein, and M. A. Despósito, Phys. Rev. E **80**, 011912 (2009).
[39] K. Laas, R. Mankin, and A. Rekker, Phys. Rev. E **79**, 051128 (2009).
[40] A. Ziehl, J. Bammert, L. Holzer, C. Wagner, and W. Zimmermann, Phys. Rev. Lett. **103**, 230602 (2009).

[41] S. V. Muniandy, W. X. Chew, and C. S. Wong, Phys. Plasmas **18**, 013701 (2011).
[42] S. Kempfle, J. Schäfer, and H. Beyer, Nonlinear Dyn. **29**, 99 (2002).
[43] V. I. Klyatskin, *Lectures on Dynamics of Stochastic Systems* (Elsevier, London, 2011).
[44] M. Gitterman, *The Noisy Oscillator: The First Hundred Years, from Einstein Until Now* (World Scientific, Singapore, 2005).
[45] V. E. Shapiro and V. M. Loginov, Physica A **91**, 563 (1978).
[46] R. C. Bourret, U. Frisch, and A. Pouquet, Physica (Utrecht) **65**, 303 (1973).